RSC Advances

PAPER

View Article Online
View Journal | View Issue

Cite this: *RSC Adv.*, 2024, **14**, 37554

Ultrasound-assisted synthesis of novel 2-aryl-3-ethoxy-5-methyl-3-oxido-2*H*-thiazolo[2,3-*e*][1,4,2]diazaphosphole-6-carboxylates and their anticancer efficacy in inducing apoptosis and autophagy and targeting cell cycle progression†

Wafa A. Bawazir,[a] Tarik E. Ali, *[bc] Mohammed A. Assiri,[c] Ali A. Shati,[d] Mohammad Y. Alfaifi[d] and Serag E. I. Elbehairi[d]

Received 5th October 2024
Accepted 11th November 2024

DOI: 10.1039/d4ra07173e

rsc.li/rsc-advances

A novel class of ethyl 2-aryl-3-ethoxy-5-methyl-3-oxido-2*H*-thiazolo[2,3-*e*][1,4,2]diazaphosphole-6-carboxylates (**2a–j**) were synthesized *via* a one-pot, three-component method. This reaction utilized ethyl 2-amino-4-methylthiazole-5-carboxylate (**1**) with different aromatic aldehydes and ethyl dichlorophosphite in THF under ultrasonic irradiation, with triethylamine as an efficient catalyst at 50 °C. The reaction provided the desired products **2a–j** in high yields within a short timeframe. The cytotoxic effects of the synthesized compounds were assessed against two human cancer cell lines, lung cancer (A549) and renal cancer (TK-10), using the sulforhodamine B (SRB) assay. This evaluation revealed that products **2e**, **2h** and **2j** demonstrated significantly higher cytotoxicity against the studied cancer cells than the standard drug doxorubicin. These bioactive products notably increased the late apoptosis rate in both cell lines and demonstrated a promising high ability to arrest the cell cycle at different phases in renal TK-10 and lung A549 cancer cells. Additionally, compounds **2e**, **2h** and **2j** displayed potential for inducing autophagy.

1. Introduction

Thiazole-based compounds exhibit a wide range of effects in medicinal chemistry and are present in numerous commercially available medicines, displaying a variety of pharmacological behaviors.[1] The thiazole moiety plays a critical role as a pharmacophore, a fundamental building block for various biological compounds. Notably, it is essential for vitamin B1 (thiamine) synthesis, which supports the nervous system by enabling acetylcholine production.[2] Thiazole derivatives are present in a wide array of natural products and medications with numerous health benefits (Fig. 1). These versatile molecules can lower blood pressure, fight infections, control seizures, combat various cancers, reduce inflammation, and exhibit promising effects against viruses, oxidative damage, pain, HIV, and malaria.[3–12] The diverse biological activities of thiazole derivatives make them a fascinating area for research with significant potential to impact numerous areas of human health.

Phosphorus-containing heterocycles are interesting molecular frameworks for the synthesis of pharmacological drugs in medicinal chemistry due to their structural diversity and biocidal effects[13–15] (Fig. 2). In particular, heterophospholes are a broad family of five-membered ring molecules with a unique structure (one phosphorus and two other elements), showing significant potential in drug development. Certain isomers, such as 1,4,2- and 1,2,3-diazaphospholes, exhibit valuable bioactivities, including anti-inflammatory, antimicrobial, and anticancer properties.[16–20]

As part of our studies on heterophospholes, we recently synthesized a promising series of some 1,4,2- and 1,2,3-diazaphosphole compounds, including 1,2,4-triazolo[3,4-*e*][1,2,3]diazaphospholes (**A**),[21] 1,2,4-triazolo[5,1-*e*][1,4,2]diazaphospholes (**B**),[22] and 5-pyrazolyl-1,4,2-diazaphosphole (**C**)[23] (Fig. 3). According to our literature survey, molecular frameworks that combine 1,3-thiazole and 1,4,2-diazaphosphole rings are rare.[24–28] These structures were constructed through Hantzsch-type 3 + 2 cyclocondensation of 2-amino-thiazoles with phosphorus halides in the presence of triethylamine (Fig. 4).

[a]*Chemistry Department, Faculty of Science, King Abdulaziz University, Jeddah, Saudi Arabia*

[b]*Central Labs, King Khalid University, AlQuraa, Abha, Saudi Arabia. E-mail: tarik_elsayed1975@yahoo.com; tismail@kku.edu.sa*

[c]*Department of Chemistry, Faculty of Science, King Khalid University, AlQuraa, Abha, Saudi Arabia*

[d]*Department of Biology, Faculty of Science, King Khalid University, AlQuraa, Abha, Saudi Arabia*

† Electronic supplementary information (ESI) available. See DOI: https://doi.org/10.1039/d4ra07173e

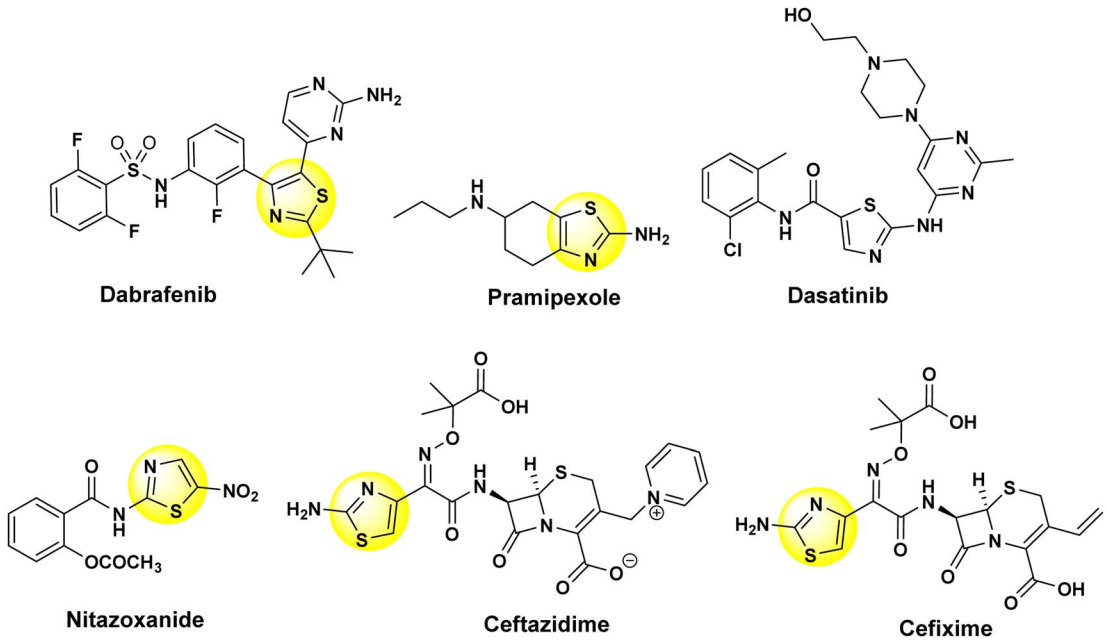

Fig. 1 Thiazole derivatives that are found in a remarkable variety of commercial drugs.

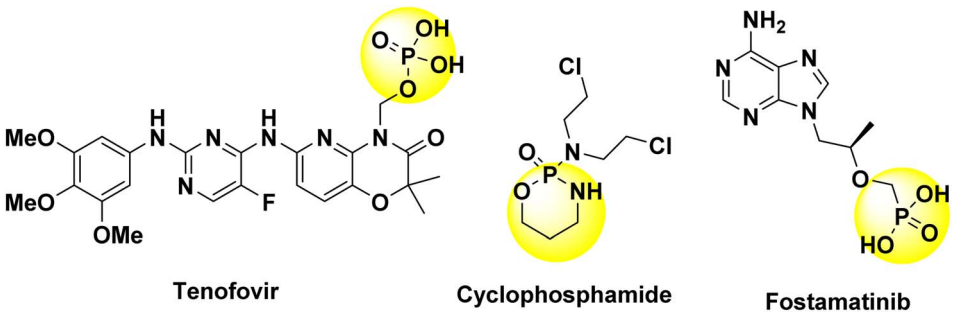

Fig. 2 Some phosphorus-containing heterocycles used in commercial drugs.

Building on the promising bioactivity observed in our exploration of novel phosphorus heterocycles,[29–32] we developed a simple and effective methodology to club the 1,4,2-diazaphosphole ring with the thiazole moiety, generating a novel class of thiazolo[2,3-*e*][1,4,2]diazaphospholes. These compounds were evaluated for their antiproliferative activities *in vitro* against two specific human cancer cell lines, lung cancer (A549) and kidney cancer (TK-10), to determine their therapeutic potential. The motivation for investigating these novel products arises from the ongoing need for new anticancer agents that can overcome the limitations of the existing therapies, such as drug resistance and toxicity. Additionally, structure–activity relationship (SAR) studies could provide insights into the optimal structural features for maximizing their

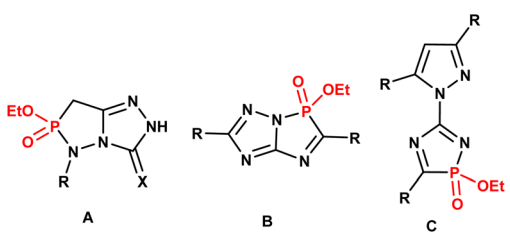

Fig. 3 Some of our recently prepared 1,4,2- and 1,2,3-diazaphosphole compounds.

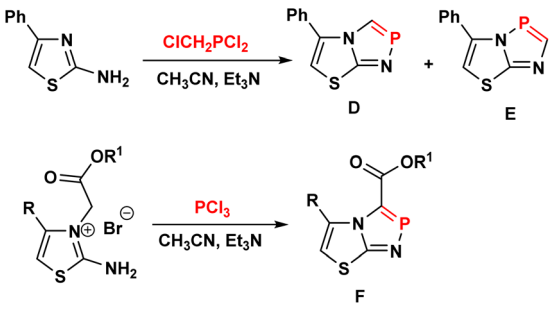

Fig. 4 Hantzsch-type 3 + 2 cyclocondensation of 2-aminothiazoles with phosphorus halides.

anticancer potency and selectivity. Ultimately, these findings aimed to inform the optimization of these compounds, leading to the development of potentially life-saving synthetic drugs.

2. Results and discussion

The synthetic strategy for designing novel ethyl 2-aryl-3-ethoxy-5-methyl-3-oxido-2*H*-thiazolo[2,3-*e*][1,4,2]diazaphosphole-6-carboxylates (**2a–j**) was achieved *via* a two-step, one-pot synthesis. The first step involved the condensation of ethyl 2-amino-4-methylthiazole-5-carboxylate (**1**)[33] with various aromatic aldehydes, forming a Schiff base. In the second step, this Schiff base reacted with ethyl dichlorophosphite under Pudovik reaction conditions. To optimize the experimental conditions, a model reaction was conducted to produce 3-ethoxy-5-methyl-2-phenyl-3-oxido-2*H*-thiazolo[2,3-*e*][1,4,2] diazaphosphole-6-carboxylate (**2a**) by reacting ethyl 2-amino-4-methylthiazole-5-carboxylate (**1**) with benzaldehyde, followed by ethyl dichlorophosphite (Scheme 1).

Initially, the reaction conducted under catalyst-free and solventless conditions produced no yield, even after 10 h at 25 °C and 60 °C (Table 1, entries 1 and 2). When basic solvents, such as DMF and pyridine, were used, the target product **2a** was formed with yields of 15% and 18%, respectively (Table 1, entries 3 and 4). We then explored the effect of various non-polar solvents, including DCM, benzene, toluene, dioxane, and THF, in the presence of equimolar amounts of various catalysts, such as K_2CO_3, DBU, and Et_3N and (Table 1, entries 5–19). Among the catalysts tested, Et_3N worked effectively, yielding the desired product **2a** in good quantities across all solvents (Table 1, entries 7, 10, 13, 16 and 19). The optimal outcome was achieved in THF, where a 75% yield was obtained with 1.0 mmol Et_3N catalyst at 60 °C (Table 1, entry 19). Increasing the amount of Et_3N to 2.0 mmol did not improve the yield further (Table 1, entry 20), but extending the reaction time from 5 to 10 h increased the yield slightly, from 75% to 78% (Table 1, entry 21). Subsequently, we aimed to perform the reaction in shorter reaction times and improved yields by using ultrasonic irradiation. Ultrasonic irradiation enhances chemical reactions by promoting cavitation, which generates high-energy microbubbles that collapse, creating localized extreme conditions (high temperature and pressure).[34,35] This accelerates reaction rates, increases the reactant surface area, and facilitates bond cleavage. It is widely used in organic synthesis, catalysis, and polymerization, offering benefits such as faster reactions, higher yields, and milder conditions.[36] Therefore, when the synthesis of product **2a** was carried out in the presence of Et_3N (1.0 mmol) under ultrasonication at room temperature, it took about 0.5 h to afford the product in a 62% yield (Table 1, entry 22). However, when the reaction was repeated under the same conditions at 50 °C for 1.5 and 3 h, it produced the final product **2a** with an improved yield of 82% (Table 1, entries 23 and 24).

Table 1 Optimization of various basic catalysts and solvents for the model reaction

Entry[a]	Catalyst	Solvent	Time (h)	Temp (°C)	Yield[b]
1	—	—	10	25	—
2	—	—	10	60	—
3	—	DMF	5	100	15%
4	—	Pyridine	5	100	18%
5	K_2CO_3 (1.0 mmol)	DCM	5	40	9%
6	DBU (1.0 mmol)	DCM	5	40	11%
7	Et_3N (1.0 mmol)	DCM	5	40	19%
8	K_2CO_3 (1.0 mmol)	Benzene	5	75	15%
9	DBU (1.0 mmol)	Benzene	5	75	18%
10	Et_3N (1.0 mmol)	Benzene	5	75	21%
11	K_2CO_3 (1.0 mmol)	Toluene	5	100	18%
12	DBU (1.0 mmol)	Toluene	5	100	20%
13	Et_3N (1.0 mmol)	Toluene	5	100	28%
14	K_2CO_3 (1.0 mmol)	Dioxane	5	100	24%
15	DBU (1.0 mmol)	Dioxane	5	100	54%
16	Et_3N (1.0 mmol)	Dioxane	5	100	63%
17	K_2CO_3 (1.0 mmol)	THF	5	60	25%
18	DBU (1.0 mmol)	THF	5	60	52%
19	Et_3N (1.0 mmol)	THF	5	60	75%
20	Et_3N (2.0 mmol)	THF	5	60	75%
21	**Et_3N (1.0 mmol)**	**THF**	**10**	**60**	**78%**
22	Et_3N (1.0 mmol)	THF	0.5	US, 25 °C	62%
23	**Et_3N (1.0 mmol)**	**THF**	**1.5**	**US, 50°C**	**82%**
24	Et_3N (1.0 mmol)	THF	3	US, 50 °C	82%

[a] Reagents: amine (**1**) (1.0 mmol) with benzaldehyde (1.0 mmol) then ethyl dichlorophosphite (1.0 mmol). [b] Yields for the isolated product.

After determining the optimal reaction conditions, an equimolar amount of triethylamine was used as a catalyst to promote the reaction, allowing all the components to couple and form the final products (**2a–j**) within 60–120 min at 50 °C in THF under ultrasonic irradiation (Scheme 2). Commercially available aldehydes with various activating or deactivating substituents were employed to yield the corresponding 2-aryl-3-ethoxy-5-methyl-3-oxido-2*H*-thiazolo[2,3-*e*][1,4,2] diazaphosphole-6-carboxylate compounds (**2a–j**). Details of the structures, yields, and reaction times for **2a–j** are provided in Scheme 2.

The proposed pathway for constructing products **2a–j** is illustrated in Scheme 3. The reaction of amine **1** with an

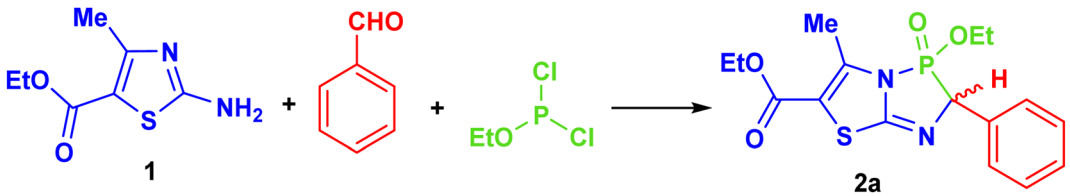

Scheme 1 Model reaction for synthesis of the target product **2a**.

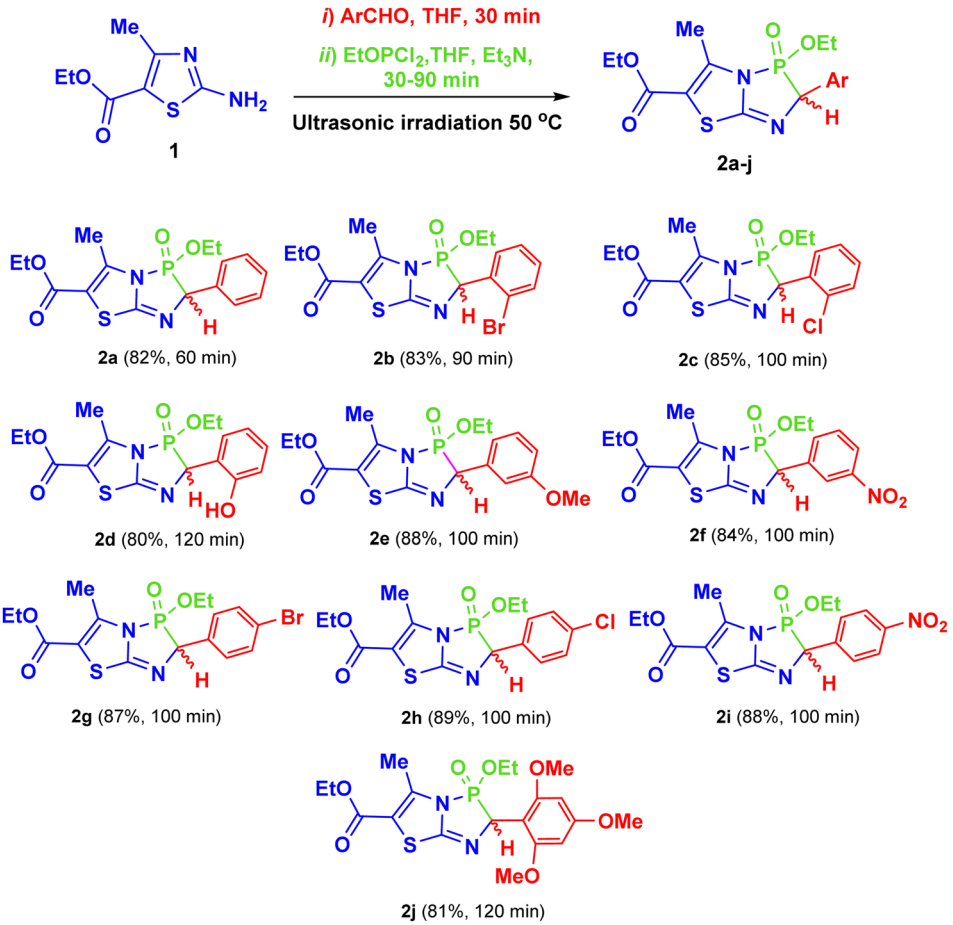

Scheme 2 Synthesis of the target products **2a–j**, and their chemical structures, reaction times and yields.

aromatic aldehyde produces intermediate **A**, as a Schiff base, through the elimination of a water molecule. Ethyl dichlorophosphite then undergoes partial hydrolysis, forming ethyl phosphonochloridate (**B**) upon the removal of water. Subsequent nucleophilic attack by intermediate **B** at the azomethine bond of **A**, catalyzed by Et_3N, leads to the formation of species **D**, which can undergo intermolecular protonation to yield the intermediate α-aminophosphonate **E**. Then, Et_3N activates the NH group of the thiazole ring in the tautomeric form **F**, facilitating an attack on the phosphorus atom and removal of a HCl molecule, ultimately affording the target products **2a–j** (Scheme 3).[37]

We confirmed the identity and structure of the target compounds **2a–j** using various physical and spectral techniques, including IR, NMR, and mass spectrometry. The IR spectra showed no NH absorption bands but displayed specific absorption bands in the regions of 1694–1707, 1263–1272, and 1014–1097 cm^{-1}, corresponding to C=O, P=O, and P–O–C functionalities, respectively. In the ^{1}H-NMR spectra, doublet chemical shifts in the range of δ 5.68–5.93 ppm were attributed to CH–P protons, with coupling constants of 17.6–22.8 Hz.[38] Quartet signals at δ 3.89–4.24 ppm were assigned to OCH_2 protons of ethoxy groups, while the singlets at δ 2.12–2.37 ppm corresponded to CH_3 protons. Additionally, triplets in the range of δ 1.03–1.29 ppm confirmed the presence of CH_3 protons in ethoxy groups. In the ^{13}C-NMR spectra, signals in the ranges of δ 13.0–15.7, 59.0–63.3, 47.5–49.8 (J_{PC} = 143–157.8 Hz), 162.8–164.9, and 166.5–168.7 ppm verified the presence of CH_3, OCH_2, CH–P, C-7a, and C=O carbons, respectively.[38] The ^{31}P-NMR chemical shifts for the synthesized compounds were within a narrow range of δ 19.52–22.52 ppm,[39] indicating the similar electronic environments for the phosphorus atoms across these compounds.

2.1 Antiproliferative properties

2.1.1 Assessment of cytotoxicity effects. To evaluate the impact of the synthesized compounds, ethyl 2-aryl-3-ethoxy-5-methyl-3-oxido-2*H*-thiazolo[2,3-*e*][1,4,2]diazaphosphole-6-carboxylate (**2a–j**), on cancer cell viability, the SRB assay[40] was conducted on two cancer cell lines: TK-10 and A549. The results were compared to the standard drug doxorubicin to evaluate the potential of the new compounds. A549 is a well-established human lung carcinoma cell line, widely used as a model for non-small cell lung cancer (NSCLC), the most common form of lung cancer. On the other hand, TK-10 is a human kidney renal adenocarcinoma cell line derived from a tumor, and is valuable for studying kidney cancer in laboratory settings. Table 2 presents the results, including the half-maximal inhibitory concentration (IC_{50}) values for each cell line, offering insights

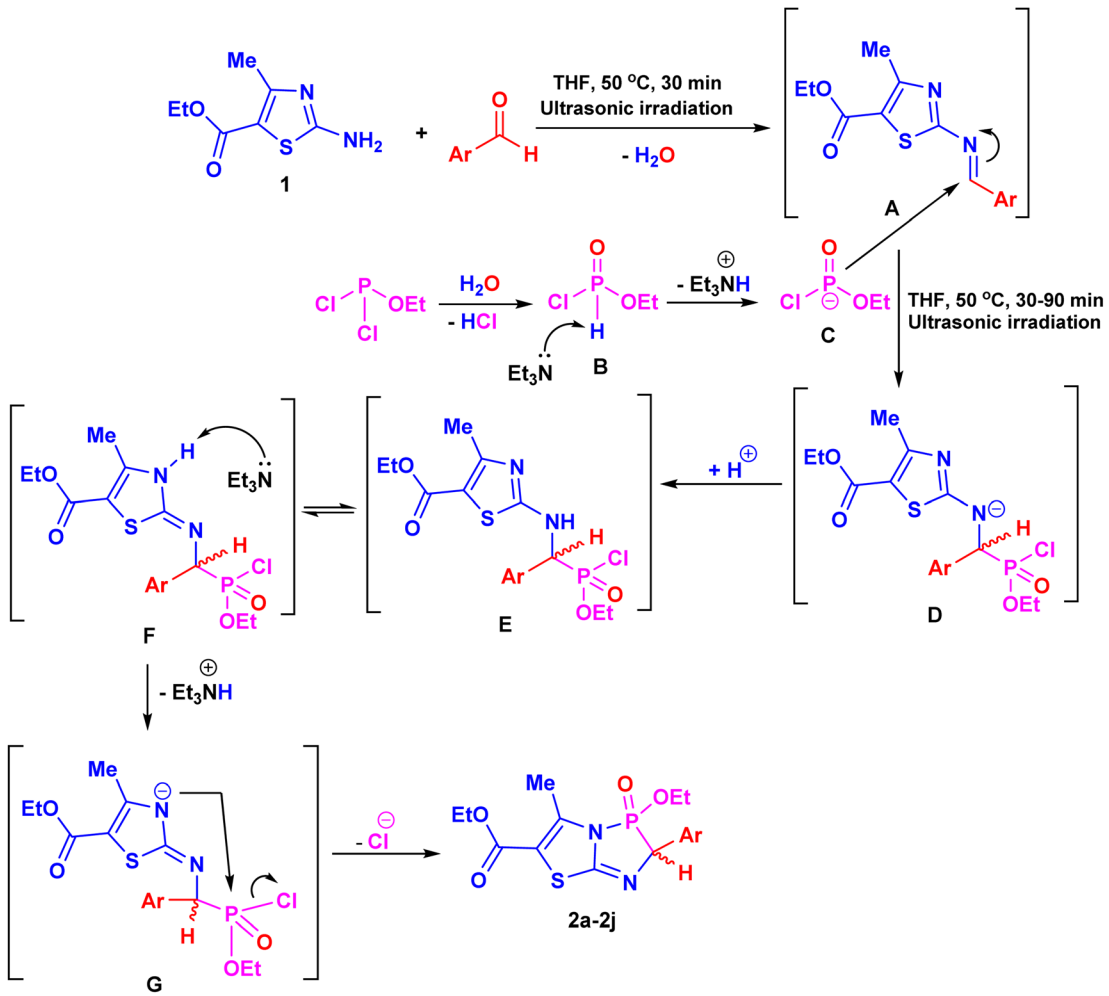

Scheme 3 The suggested reaction mechanism for the formation of the target products 2a–2j.

into the compounds' effectiveness. The National Cancer Institute considers an IC_{50} value of ≤ 10 μg mL^{-1} as a benchmark for potential anticancer efficacy. In the case of TK-10 human kidney renal cancer cells, the growth data showed that compounds **2e**, **2g**, **2h**, and **2j** exhibited strong cytotoxic activity, effectively suppressing cancer cell growth. Their IC_{50} values ranged from 1.0 ± 0.1 to 5.1 ± 0.7 μg mL^{-1}. While the standard drug doxorubicin also inhibited cancer cell growth, it showed an IC_{50} value of 1.4 ± 0.4 μg mL^{-1} compared to these compounds. In contrast, compounds **2a**, **2b**, **2f**, and **2i** were ineffective, requiring higher concentrations to inhibit cell proliferation. Compound **2c** showed some potential anticancer activity, with an IC_{50} of 11.7 ± 2.3 μg mL^{-1}, though it was less potent than the other active compounds. Compounds **2e**, **2g**, **2h**, and **2j** demonstrated remarkable cytotoxicity against A549 human lung cancer cells, achieving over 50% growth inhibition at very low concentrations (1.0 ± 0.1 to 10.9 ± 1.2 μg mL^{-1}). In contrast, the other synthesized compounds **2a**, **2b**, **2c**, **2f**, and **2i** were inactive, requiring higher concentrations than doxorubicin to achieve similar effects. Therefore, compounds **2e**, **2h**, and **2j** showed promising cytotoxicity against lung cancer cells and warrant further investigation as potential candidates for developing new treatments for both kidney and lung cancers.

Table 2 *In vitro* anticancer activity of the products 2a–j against TK-10 and A549 cancer cells

	IC_{50} (μg mL^{-1})	
Compounds	TK-10	A549
2a	≥100	≥100
2b	≥100	66.9 ± 0.7
2c	11.7 ± 2.3	33.4 ± 0.8
2d	≥100	≥100
2e	**1.0 ± 0.1**	**2.4 ± 0.3**
2f	≥100	≥100
2g	5.1 ± 0.7	10.9 ± 1.2
2h	**2.3 ± 0.1**	**4.7 ± 0.2**
2i	≥100	44.7 ± 3.6
2j	**1.4 ± 0.1**	**1.0 ± 0.1**
Doxorubicin	1.4 ± 0.4	1.9 ± 0.7

2.1.2 Study of the structure–activity relationship (SAR). The combination of a 1,4,2-diazaphosphole ring and a thiazole ring within a single molecular framework exhibited variable cytotoxic effects in most products, depending on the type of

substituted aryl group. The data suggested that these functional groups play a significant role in influencing the compounds' potency against the tested cell lines.

• The existence of any substituent at the phenyl ring in most compounds **2b–j** caused cytotoxic effects in comparison with compound **2a** against the two cancer cell lines.

• The presence of *ortho*-substituted groups in compounds **2b** (2-Br), **2c** (2-Cl), and **2d** (2-HO) generally exhibited lower IC_{50} values against A549 cells. This suggested that steric effects in the *ortho* position may hinder effective binding.

• The presence of *meta*-substituted groups, as in compound **2e** (3-MeO), significantly enhanced the bioactivity. Compound

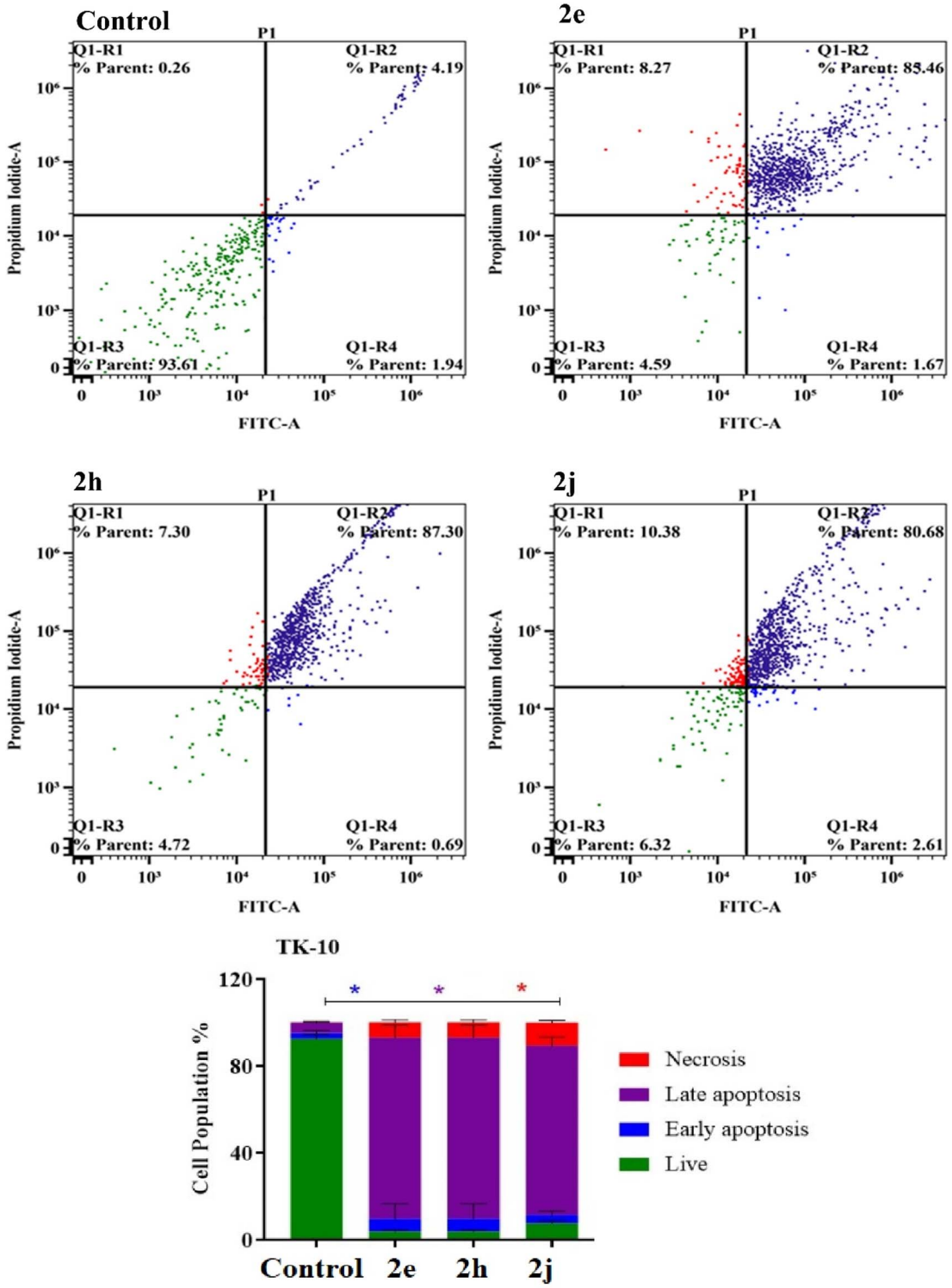

Fig. 5 Apoptosis/necrosis assessment of the products **2e**, **2h** and **2j** against the TK-10 cell lines.

2e had among the lowest IC_{50} values (2.4 μg mL^{-1} for A549 cells and 1.0 μg mL^{-1} for TK-10 cells), indicating that a *meta*-positioned electron-donating group (MeO) is highly favorable for potency.

• The presence of *para*-substituted halogens in compounds **2g** (4-Br) and **2h** (4-Cl) also improved the activity, although they were less potent than *meta*-substituted **2e** (3-MeO).

• The existence of nitro groups in any position, as in both products **2f** and **2i**, appeared to reduce the cytotoxic effects, as

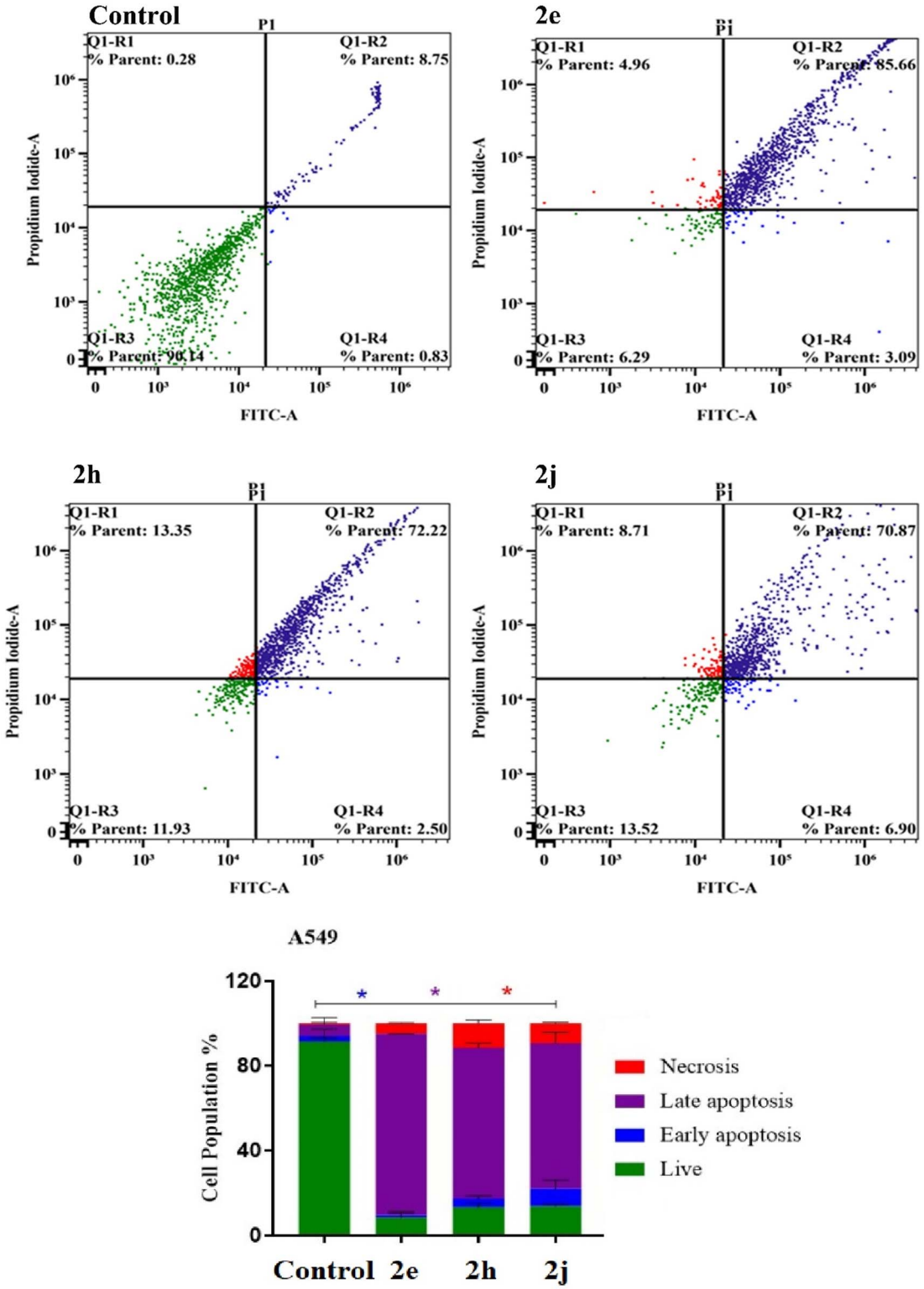

Fig. 6 Apoptosis/necrosis assessment of the products **2e**, **2h** and **2j** against the A549 cell lines.

these compounds had IC_{50} values $\geq 100\ \mu g\ mL^{-1}$ for at least one of the cell lines.

• Halogen-substituted compounds, such as **2b**, **2c**, **2g**, and **2h**, may be effective in improving the cytotoxic effect, especially when they are in the *para*-position.

• Both products **2e** and **2j** showed IC_{50} values that were close to doxorubicin, indicating their strong anticancer activities. This suggested that a single *meta*-positioned methoxy or multiple methoxy groups may be effective modifications to optimize the potency.

• We can hypothesize the potential mechanisms based on the structural features. The different aromatic rings and planar structures in these products can often intercalate into DNA, disrupting replication and transcription processes, which is

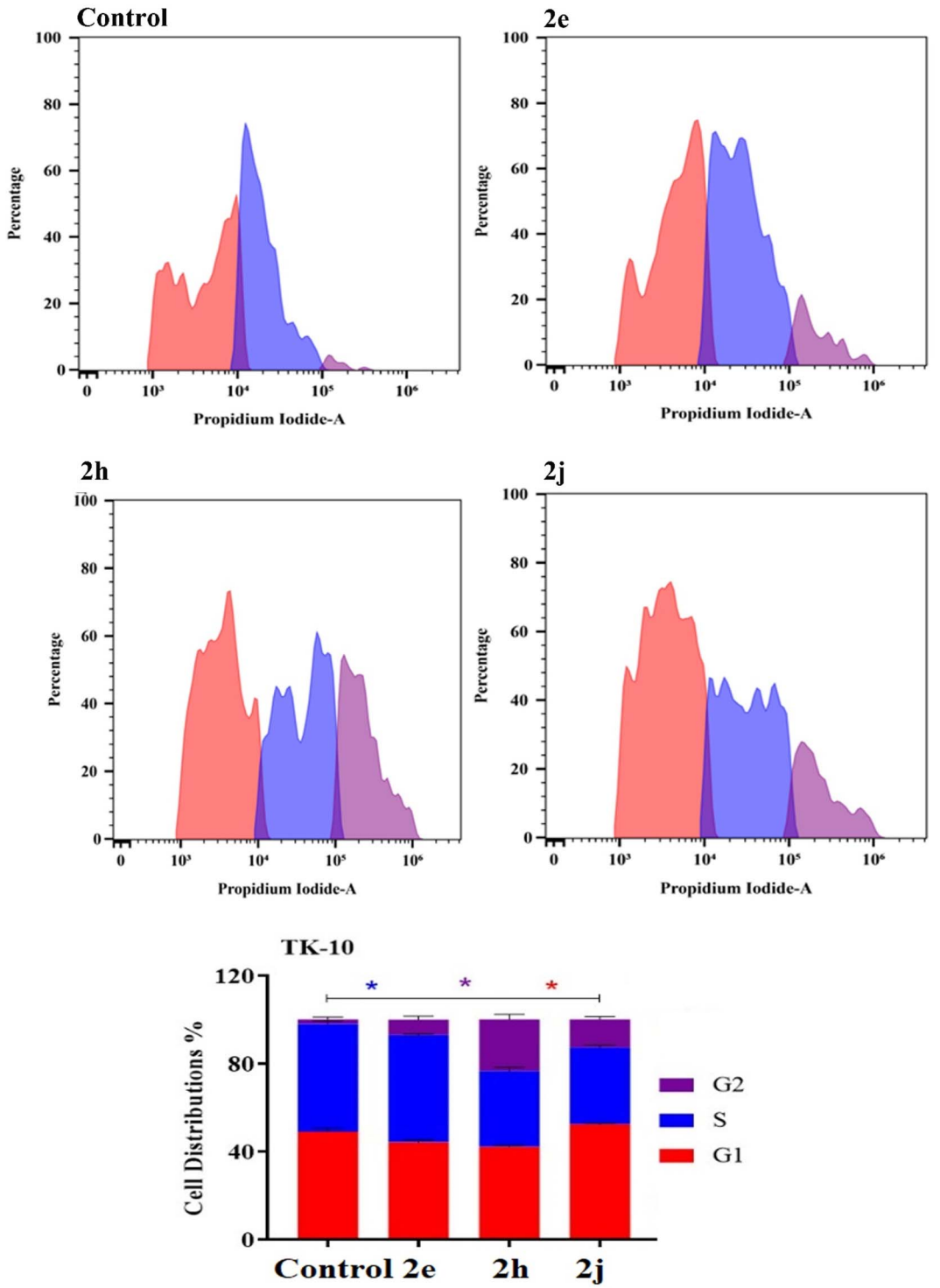

Fig. 7 Cell cycle distribution determined using DNA cytometry analysis of the products **2e**, **2h** and **2j** against the TK-10 cell lines.

common in anticancer agents. In addition, the products that have halogen and methoxy substituents could interact with specific cell receptors or enzymes, potentially inhibiting pathways critical to cancer cell survival and proliferation.

2.1.3 Apoptosis analysis. To investigate the apoptotic activity of the bioactive compounds **2e**, **2h**, and **2j**, we analyzed and quantified the percentage of apoptotic cells using Alexa Fluor-488/PI staining, followed by flow cytometric analysis.[41] The data revealed a significant increase in late apoptosis in TK-10 lung cancer cells treated with **2e**, **2h**, and **2j**, with annexin-V quantification showing 85.46%, 87.30%, and 80.68% apoptotic cells, respectively, compared to the control (4.19%), alongside mild changes in early apoptosis. More notably, compounds **2e**, **2h**, and **2j** effectively reduced the percentage of viable cells to

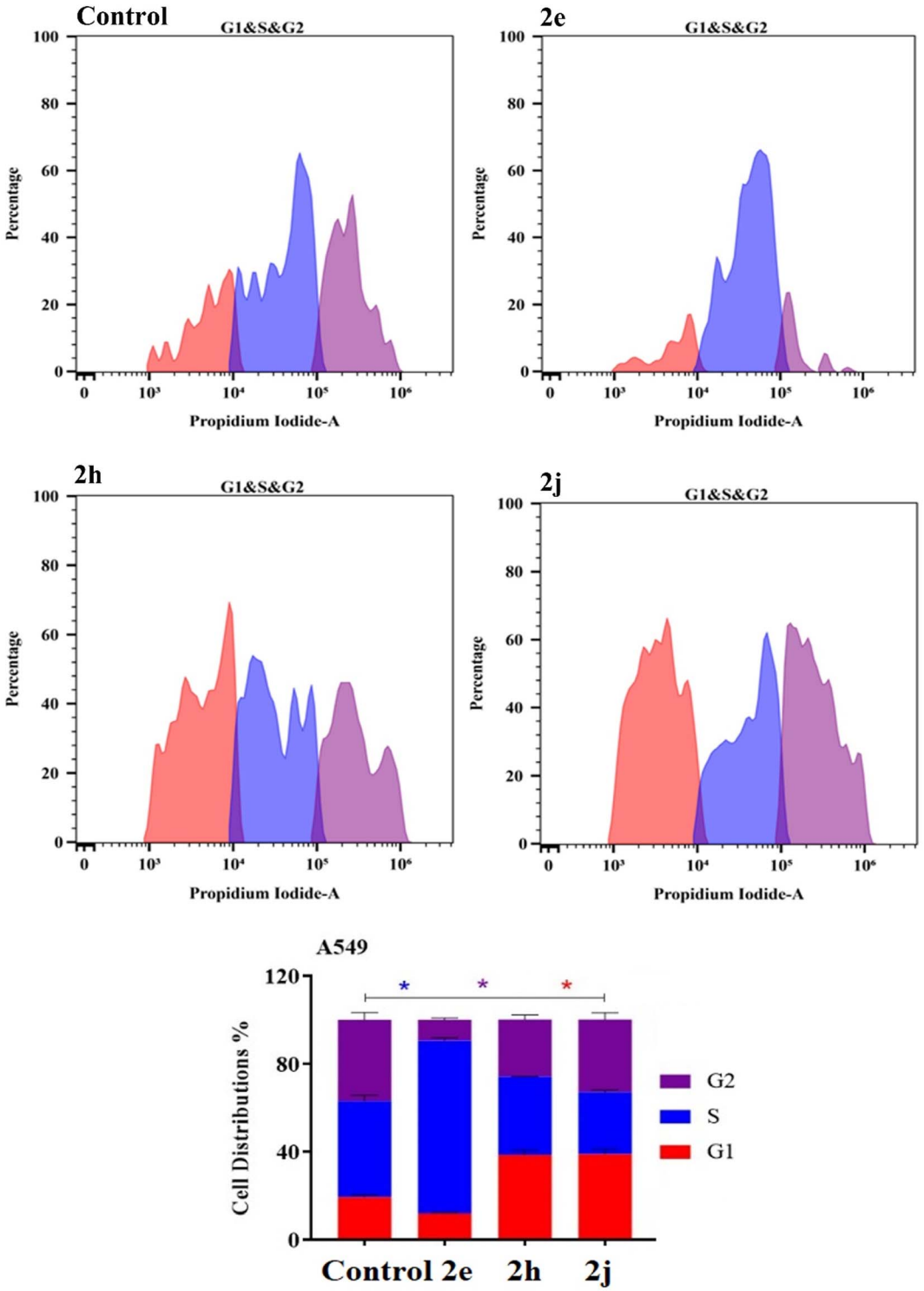

Fig. 8 Cell cycle distribution determined using DNA cytometry analysis of the products **2e**, **2h** and **2j** against the A549 cell lines.

4.59%, 4.72%, and 6.32%, respectively, compared to the control (93.61%) (Fig. 5). Consistently, the necrotic cell populations in TK-10 cells treated with these compounds were significantly higher, ranging from 7.30% to 10.38%. Similarly, in A549 renal cancer cells, compounds **2e**, **2h**, and **2j** induced a significant increase in late apoptosis (85.66%, 72.22%, and 70.87%, respectively) compared to the control (8.75%). Furthermore, these compounds significantly increased the necrotic cell populations (4.96%, 13.35%, and 8.71%) relative to the control (0.28%) and reduced cellular viability (Fig. 6). These results supported that compounds **2e**, **2h**, and **2j** exert their cytotoxic effects on both TK-10 lung and A549 renal cancer cells by enhancing late apoptosis and reducing cellular viability.

2.1.4 Cell cycle distribution. To evaluate the potential activity of the bioactive compounds **2e**, **2h**, and **2j**, we examined their effects on the cell cycle of TK-10 and A549 cancer cells using standard flow cytometry.[42] In TK-10 lung cancer cells, our results demonstrated that compounds **2e**, **2h**, and **2j**, induced cell cycle arrest at the G1 phase, with average percentages of 44.28%, 42.13%, and 52.46%, respectively, compared to the control group (49.1%). Our data also showed that these compounds did not cause cell cycle arrest at the S phase relative to the control. Moreover, compounds **2e**, **2h**, and **2j** significantly increased cellular accumulation and cell cycle arrest at the G2 phase, with respective percentages of 7.09%, 23.34%, and 12.74%, compared to the control (1.90%) (Fig. 7). In A549 renal cancer cells, the analysis indicated that compounds **2h** and **2j** significantly arrested the cell cycle at the G1 phase (38.75% and 38.97%, respectively) compared to the control (19.33%). Compound **2e** showed a non-significant effect on arresting cell distribution at the S phase, with a percentage of 78.66% relative to the control (43.87%). Additionally, compounds **2h** and **2j** arrested the cell cycle at the S phase at lower percentages (35.59% and 28.14%, respectively) compared to the control (43.87%). For compound **2e**, cellular accumulation was notably decreased at the G2 phase, with cell cycle arrest also observed for compounds **2h** and **2j** (Fig. 8). In summary, compounds **2e**, **2h**, and **2j** exhibited promising potential for inducing cell cycle arrest at the G1, S, and G2 phases in TK-10 lung and A549 renal cancer cells.

2.1.5 Autophagy assessment. We investigated the impact of the bioactive compounds **2e**, **2h**, and **2j** on cancer cells by focusing on autophagy, a cellular self-cleaning process. Acridine orange staining, combined with flow cytometry, was used to track the formation of acidic vesicular organelles (AVOs) associated with autophagy.[43] The percentage of net fluorescent intensity (NFI) for AVO formation was calculated after exposure to the pre-determined IC_{50} values of compounds **2e**, **2h**, and **2j**. In TK-10 cells, compounds **2e**, **2h**, and **2j** significantly induced AVO formation at the tested doses, with increases of 36.1%, 42.2%, and 53.4%, respectively, compared to the control (31.9%) (Fig. 9). Similarly, in A549 cells, these compounds induced significant increases in autophagic signals by 47.6%, 32.9%, and 58.0%, respectively (Fig. 10). These findings suggested that compounds **2e**, **2h**, and **2j** have the potential to activate both autophagic and apoptotic cell death pathways in cancer cells.

3. Experimental

The melting points were measured using a digital Stuart SMP-3 apparatus in open capillary tubes. Infrared spectroscopy (FT-IR) was performed using a Nicolet iS10 spectrophotometer. Nuclear magnetic resonance (NMR) analysis, comprising ^{1}H, ^{13}C, and ^{31}P NMR spectroscopies, was performed on a Bruker 400 MHz spectrometer in deuterated dimethyl sulfoxide (DMSO-d_6) at 400, 100, and 162 MHz, respectively, with tetramethyl silane (TMS) as the internal standard. Mass spectrometry was performed using a single quadrupole mass analyzer (Thermo Scientific GCMS) with a direct probe controller inlet. The purity of the synthesized compounds was confirmed using thin-layer chromatography (TLC), while their elemental composition was determined by analysis with a PerkinElmer 2400II instrument. For ultrasonic irradiation, an Elmasonic S 60 (H) (ultrasonic frequency 37 MHz, power 60 W) ultrasound bath was used, and the reaction flask was located in the ultrasonic bath containing water.

3.1 Syntheses of 2-phenyl-3-ethoxy-5-methyl-3-oxido-2*H*-thiazolo[2,3-*e*][1,4,2]diazaphosphole-6-carboxylate (2a–2j)

3.1.1 Method 1 (conventional thermal heating). A mixture of ethyl 2-amino-4-methylthiazole-5-carboxylate (**1**) (2.5 mmol, 0.46 g) and an aromatic aldehyde (2.5 mmol) was dissolved in tetrahydrofuran (20 mL). The reaction was carried out by heating under reflux for 2 h. Subsequently, a solution of ethyl dichlorophosphite (2.5 mmol, 0.29 mL) in THF (5 mL) with triethylamine (2.5 mmol, 0.34 mL) was added dropwise to the reaction mixture. The mixture was then heated under reflux at 60 °C for an additional 8 h. After completion, the reaction mixture was cooled to room temperature, and the solvent was removed under reduced pressure. The residue was dissolved in ethyl acetate (50 mL) and washed with water (3 × 50 mL) to remove water-soluble byproducts. The organic phase was separated, dried over anhydrous sodium sulfate, and concentrated under reduced pressure. The crude product was then purified by column chromatography using a hexane/ethyl acetate (1 : 2) elution system, yielding the purified product.

3.1.2 Method 2 (ultrasonic irradiation). A mixture of ethyl 2-amino-4-methylthiazole-5-carboxylate (**1**) (2.5 mmol, 0.46 g) and an aromatic aldehyde (2.5 mmol) was dissolved in tetrahydrofuran (20 mL). The reaction mixture was then exposed to ultrasound irradiation for 30 min. Following this, a solution of ethyl dichlorophosphite (2.5 mmol, 0.29 mL) in THF (5 mL), along with triethylamine (2.5 mmol, 0.34 mL), was added gradually to the reaction mixture. The resulting mixture was further subjected to ultrasound irradiation at 50 °C for an additional 30–90 min. Upon completion, the reaction mixture was cooled to room temperature, and the solvent was evaporated under reduced pressure. The residue was dissolved in ethyl acetate (50 mL) and washed with water (3 × 50 mL) to remove water-soluble byproducts. The organic layer was separated, dried over anhydrous sodium sulfate, and concentrated under reduced pressure. The crude product was purified by column chromatography using a hexane/ethyl acetate (1 : 2) elution system, yielding the purified product.

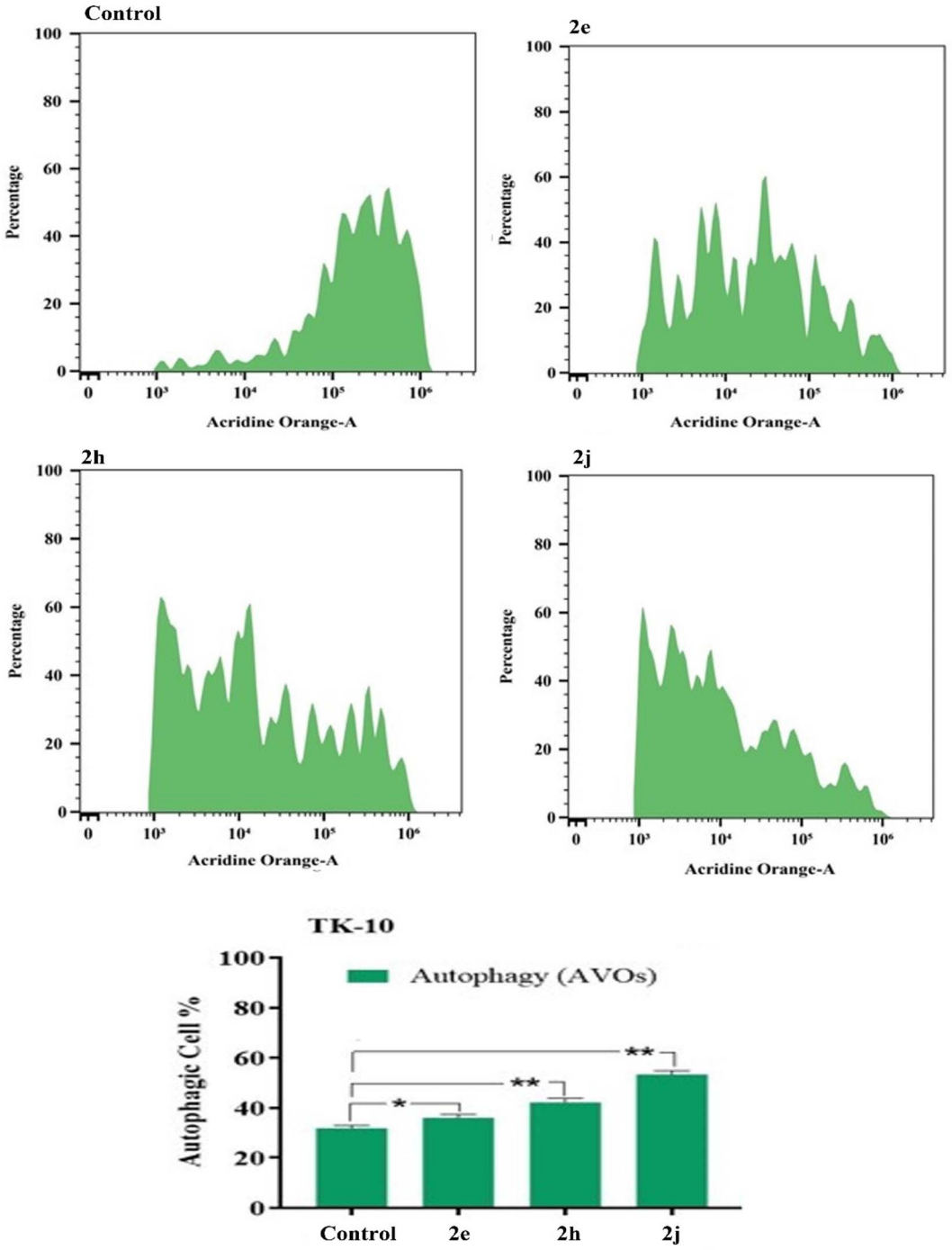

Fig. 9 Autophagic cell death assessment in TK-10 cell lines to compounds **2e**, **2h** and **2j**.

3.1.3 3-Ethoxy-5-methyl-2-phenyl-3-oxido-2*H*-thiazolo[2,3-*e*][1,4,2]diazaphosphole-6-carboxylate (2a). White solid obtained after 90 min in an 82% yield (0.74 g), mp 182–183 °C. IR (KBr), (ν max, cm^{-1}): 3040 (C–H_{arom}), 2982, 2943, 2905 (C–H_{aliph}), 1707 (C=O), 1268 (P=O), 1088, 1043, 1017 (P–O–C and O–C). ^{1}H-NMR (400 MHz, DMSO-d_6): 1.06 (t, 3H, J = 7.2 Hz, CH_3), 1.26 (t, 3H, J = 7.2 Hz, CH_3), 2.33 (s, 3H, CH_3), 3.99 (q, 2H, J = 7.2 Hz, OCH_2), 4.21 (q, 2H, J = 7.2 Hz, OCH_2), 5.82 (d, 1H, J_{PCH} = 20.4 Hz, P–CH), 7.15 (d, 2H, J = 7.2 Hz, Ph–H), 7.37–7.45 (m, 3H, Ph–H). ^{13}C-NMR (100 MHz, DMSO-d_6): 13.0 (CH_3), 14.2 (CH_3), 15.1 (CH_3), 47.5 (d, J_{PC} = 143.0 Hz, C-2), 62.3 (OCH_2), 63.3 (OCH_2), 125.4 (C-4_{phenyl}), 129.4 (C-$3,5_{phenyl}$), 130.1 (C-$2,6_{phenyl}$), 137.0 (C-1_{phenyl}), 139.6 (C-6), 153.7 (C-5), 164.9 (C-7a), 168.4 (C=O). ^{31}P-NMR (162 MHz, DMSO-d_6): 22.25 ppm. MS (m/z, I%): 366 (M^+, 18%). Anal. calcd for $C_{16}H_{19}N_2O_4PS$ (366.37): C, 52.45%; H, 5.23%; N, 7.65%; S, 8.75%. Found: C, 52.34%; H, 5.16%; N, 7.49%; S, 8.61%.

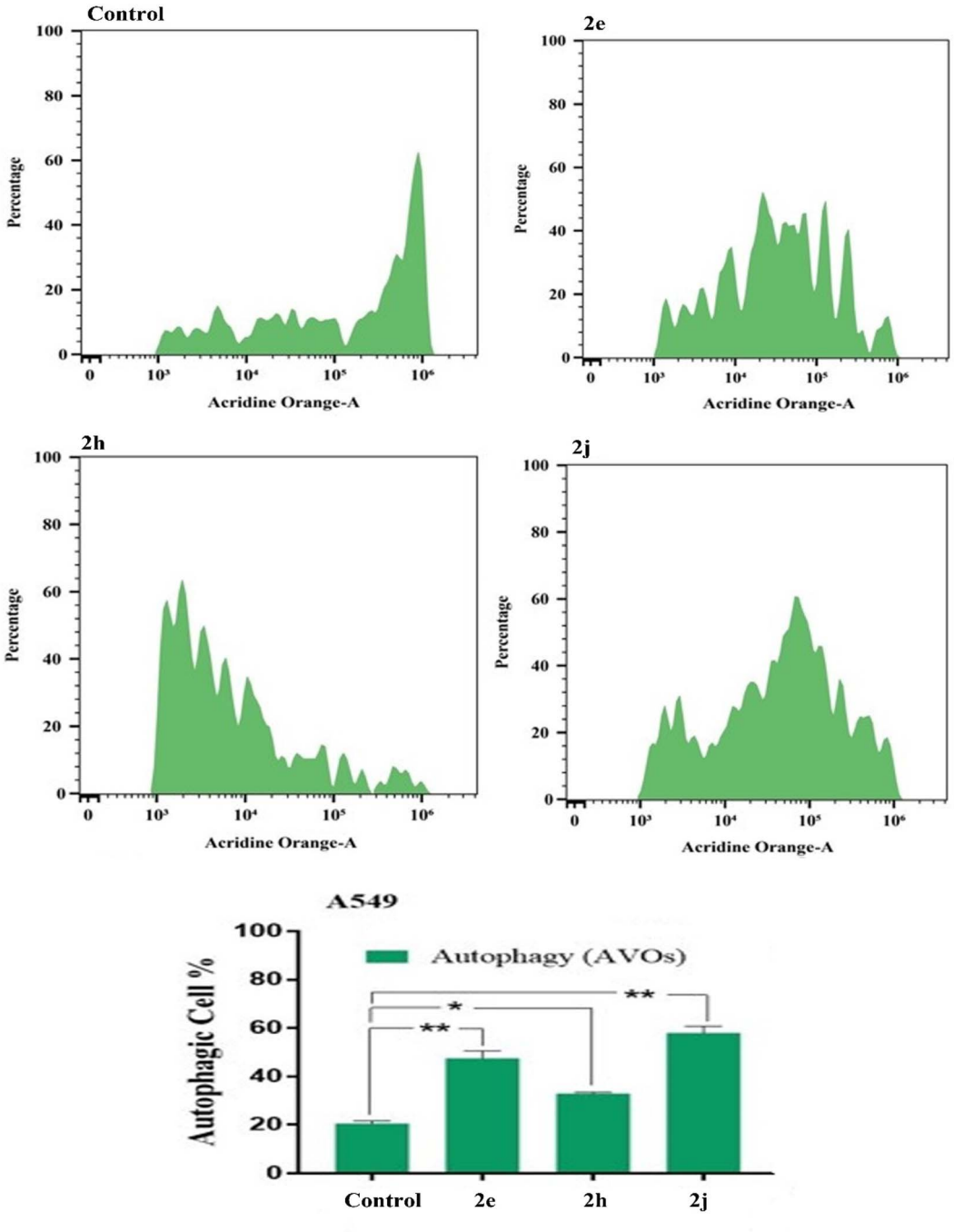

Fig. 10 Autophagic cell death assessment in TK-10 cell lines to compounds **2e**, **2h** and **2j**.

3.1.4 2-(2-Bromophenyl)-3-ethoxy-5-methyl-3-oxido-2*H*-thiazolo[2,3-*e*][1,4,2]diazaphosphole-6-carboxylate (2b). Yellow solid obtained after 90 min in an 83% yield (0.91 g), mp 192–194 °C. IR (KBr), (ν max, cm^{-1}): 3090 ($C–H_{arom}$), 2979, 2926, 2899 ($C–H_{aliph}$), 1698 (C═O), 1269 (P═O), 1097, 1038 (P–O–C and O–C). ^{1}H-NMR (400 MHz, DMSO-d_6): 1.06 (t, 3H, $J = 7.2$ Hz, CH_3), 1.23 (t, 3H, $J = 7.6$ Hz, CH_3), 2.20 (s, 3H, CH_3), 3.92 (q, 2H, $J = 7.2$ Hz, OCH_2), 4.13 (q, 2H, $J = 6.8$ Hz, OCH_2), 5.79 (d, 1H, $J_{PCH} = 17.6$ Hz, P–CH), 7.39–7.7.47 (m, 2H, Ar–H), 7.72 (t, 1H, $J =$ 7.2 Hz, Ar–H), 7.90 (d, 1H, $J = 7.2$ Hz, Ar–H). ^{13}C-NMR (100 MHz, DMSO-d_6): 13.1 (CH_3), 15.3 (CH_3), 16.1 (CH_3), 48.5 (d, $J_{PC} =$ 148.7 Hz, C-2), 59.0 (OCH_2), 60.4 (OCH_2), 124.3 ($C\text{-}2_{aryl}$), 126.9 ($C\text{-}5_{aryl}$), 127.7 ($C\text{-}4_{aryl}$), 131.3 ($C\text{-}6_{aryl}$), 132.1 ($C\text{-}3_{aryl}$), 137.9 (C-6), 141.5 ($C\text{-}1_{aryl}$), 155.5 (C-5), 164.1 (C-7a), 167.5 (C═O). ^{31}P-NMR (162 MHz, DMSO-d_6): 20.25 ppm. MS (m/z, I%): 444 (M^+, 27%) and 446 (M + 2, 18%). Anal. calcd for $C_{16}H_{18}BrN_2O_4PS$ (445.27): C, 43.16%; H, 4.07%; N, 6.29%; S, 7.20%. Found: C, 43.04%; H, 3.92%; N, 6.13%; S, 7.10%.

3.1.5 2-(2-Chlorophenyl)-3-ethoxy-5-methyl-3-oxido-2*H*-thiazolo[2,3-*e*][1,4,2]diazaphosphole-6-carboxylate (2c). Yellow solid obtained after 100 min in an 85% yield (0.84 g), mp 186–188 °C. IR (KBr), (ν max, cm^{-1}): 3053 ($C–H_{arom}$), 2979, 2943,

2911 (C–H_{aliph}), 1704 (C=O), 1268 (P=O), 1082, 1042 (P–O–C and O–C). ^{1}H-NMR (400 MHz, DMSO-d_6): 1.07 (t, 3H, J = 6.4 Hz, CH_3), 1.23 (t, 3H, J = 6.8 Hz, CH_3), 2.21 (s, 3H, CH_3), 3.93 (q, 2H, J = 7.2 Hz, OCH_2), 4.24 (q, 2H, J = 6.4 Hz, OCH_2), 5.82 (d, 1H, J_{PCH} = 20.8 Hz, P–CH), 7.42 (t, 1H, J = 7.2 Hz, Ar–H), 7.50 (t, 1H, J = 7.2 Hz, Ar–H), 7.91 (d, 1H, J = 7.6 Hz, Ar–H), 8.04 (d, 1H, J = 8.0 Hz, Ar–H). ^{13}C-NMR (100 MHz, DMSO-d_6): 13.5 (CH_3), 15.6 (CH_3), 16.3 (CH_3), 48.4 (d, J_{PC} = 148.6 Hz, C-2), 60.5 (OCH_2), 61.6 (OCH_2), 125.8 (C-5_{aryl}), 126.9 (C-4_{aryl}), 128.1 (C-3_{aryl}), 130.5 (C-6_{aryl}), 133.3 (C-2_{aryl}), 135.5 (C-1_{aryl}), 138.4 (C-6), 154.6 (C-5), 164.4 (C-7a), 168.7 (C=O). ^{31}P-NMR (162 MHz, DMSO-d_6): 20.03 ppm. MS (m/z, I%): 399 (M^+, 9%) and 401 (M^+, 3%). Anal. calcd for $C_{16}H_{18}ClN_2O_4PS$ (400.81): C, 47.95%; H, 4.53%; N, 6.99%; S, 8.00%. Found: C, 47.83%; H, 4.42%; N, 6.89%; S, 7.85%.

3.1.6 3-Ethoxy-2-(4-hydroxyphenyl)-5-methyl-3-oxido-2*H*-thiazolo[2,3-*e*][1,4,2]diazaphosphole-6-carboxylate (2d). Yellow solid obtained after 120 min in an 80% yield (0.75 g), mp 175–176 °C. IR (KBr), (ν max, cm^{-1}): 3208 (OH), 3032 (C–H_{arom}), 2984, 2940, 2908 (C–H_{aliph}), 1698 (C=O), 1267 (P=O), 1091, 1016 (P–O–C and O–C). ^{1}H-NMR (400 MHz, DMSO-d_6): 1.16 (t, 3H, J = 6.8 Hz, CH_3), 1.22 (t, 3H, J = 7.2 Hz, CH_3), 2.39 (s, 3H, CH_3), 4.02 (q, 2H, J = 7.2 Hz, OCH_2), 4.21 (t, 2H, J = 6.8 Hz, OCH_2), 5.93 (d, 1H, J_{PCH} = 20.4 Hz, P–CH), 6.82 (t, 2H, J = 7.2 Hz, Ar–H), 7.11 (d, 1H, J = 7.2 Hz, Ar–H), 7.43 (d, 1H, J = 7.6 Hz, Ar–H), 9.07 (brs, 1H, OH). ^{13}C-NMR (100 MHz, DMSO-d_6): 13.5 (CH_3), 15.6 (CH_3), 16.4 (CH_3), 48.1 (d, J_{PC} = 151.4 Hz, C-2), 60.4 (OCH_2), 62.2 (OCH_2), 116.5 (C-3_{aryl}), 121.2 (C-5_{aryl}), 125.8 (C-1_{aryl}), 128.8 (C-4_{aryl}), 129.0 (C-6_{aryl}), 138.4 (C-6), 154.6 (C-5), 157.5 (C-2_{aryl}), 163.6 (C-7a), 167.0 (C=O). ^{31}P-NMR (162 MHz, DMSO-d_6): 20.02 ppm. MS (m/z, I%): 382 (M^+, 6%). Anal. calcd for $C_{16}H_{19}N_2O_5PS$ (382.37): C, 50.26%; H, 5.01%; N, 7.33%; S, 8.38%. Found: C, 50.08%; H, 4.92%; N, 7.18%; S, 8.22%.

3.1.7 3-Ethoxy-3-(3-methoxyphenyl)-5-methyl-3-oxido-2*H*-thiazolo[2,3-*e*][1,4,2]diazaphosphole-6-carboxylate (2e). Yellow solid obtained after 100 min in an 88% yield (0.86 g), mp 167–169 °C. IR (KBr), (ν max, cm^{-1}): 3067 (C–H_{arom}), 2979, 2940, 2905 (C–H_{aliph}), 1707 (C=O), 1268 (P=O), 1083, 1041 (P–O–C and O–C). ^{1}H-NMR (400 MHz, DMSO-d_6): 1.03 (t, 3H, J = 6.4 Hz, CH_3), 1.23 (t, 3H, J = 7.2 Hz, CH_3), 2.12 (s, 3H, CH_3), 3.71 (s, 3H, OCH_3), 3.92 (q, 2H, J = 7.2 Hz, OCH_2), 4.21 (q, 2H, J = 6.8 Hz, OCH_2), 5.82 (d, 1H, J_{PCH} = 21.2 Hz, P–CH), 7.43 (t, 1H, J = 7.2 Hz, Ar–H), 7.71 (d, 1H, J = 8.00 Hz, Ar–H), 7.91 (d, 1H, J = 7.6 Hz, Ar–H), 8.43 (s, 1H, Ar–H). ^{13}C-NMR (100 MHz, DMSO-d_6): 13.7 (CH_3), 14.8 (CH_3), 15.9 (CH_3), 48.0 (d, J_{PC} = 152.6 Hz, C-2), 54.3 (OCH_3), 59.3 (OCH_2), 61.9 (OCH_2), 115.5 (C-4_{aryl}), 116.6 (C-2_{aryl}), 121.5 (C-6_{aryl}), 123.4 (C-5_{aryl}), 137.1 (C-1_{aryl}), 139.5 (C-6), 156.0 (C-5), 159.0 (C-3_{aryl}), 162.8 (C-7a), 166.7 (C=O). ^{31}P-NMR (162 MHz, DMSO-d_6): 19.52 ppm. MS (m/z, I%): 396 (M^+, 43%). Anal. calcd for $C_{17}H_{21}N_2O_5PS$ (396.40): C, 51.51%; H, 5.34%; N, 7.07%; S, 8.09%. Found: C, 51.34%; H, 5.31%; N, 6.95%; S, 7.96%.

3.1.8 3-Ethoxy-5-methyl-2-(3-nitrophenyl)-3-oxido-2*H*-thiazolo[2,3-*e*][1,4,2]diazaphosphole-6-carboxylate (2f). Pale yellow solid obtained after 100 min in an 84% yield (0.85 g), mp 218–220 °C. IR (KBr), (ν max, cm^{-1}): 3067, 3035 (C–H_{arom}), 2987, 2931, 2905, 2870 (C–H_{aliph}), 1701 (C=O), 1270 (P=O), 1097, 1044, 1014 (P–O–C and O–C). ^{1}H-NMR (400 MHz, DMSO-d_6): 1.10 (t, 3H, J = 6.8 Hz, CH_3), 1.14–1.23 (m, 3H, CH_3), 2.38 (s, 3H, CH_3), 3.89–4.16 (m, 4H, OCH_2), 5.72 (dd, 1H, J_{PCH} = 22.0 and 9.2 Hz, P–CH), 7.69 (t, 1H, J = 7.6 Hz, Ar–H), 8.18 (d, 1H, J = 7.2 Hz, Ar–H), 8.33 (d, 1H, J = 7.2 Hz, Ar–H), 8.39 (s, 1H, Ar–H). ^{13}C-NMR (100 MHz, DMSO-d_6): 13.2 (CH_3), 14.3 (CH_3), 15.2 (CH_3), 47.9 (d, J_{PC} = 157.8 Hz, C-2), 60.1 (OCH_2), 61.9 (OCH_2), 125.1 (C-2_{aryl}), 128.5 (C-4_{aryl}), 129.4 (C-5_{aryl}), 135.6 (C-6_{aryl}), 137.4 (C-6), 139.4 (C-1_{aryl}), 143.5 (C-3_{aryl}), 154.2 (C-5), 163.1 (C-7a), 167.4 (C=O). ^{31}P-NMR (162 MHz, DMSO-d_6): 20.06 ppm. MS (m/z, I%): 411 (M^+, 51%). Anal. calcd for $C_{16}H_{18}N_3O_6PS$ (411.37): C, 46.72%; H, 4.41%; N, 10.21%; S, 7.79%. Found: C, 46.58%; H, 4.31%; N, 10.09%; S, 7.67%.

3.1.9 2-(4-Bromophenyl)-3-ethoxy-5-methyl-3-oxido-2*H*-thiazolo[2,3-*e*][1,4,2]diazaphosphole-6-carboxylate (2g). Pale yellow solid obtained after 100 min in an 87% yield (0.95 g), mp 196–197 °C. IR (KBr), (ν max, cm^{-1}): 3038 (C–H_{arom}), 2987, 2980, 2927 (C–H_{aliph}), 1703 (C=O), 1271 (P=O), 1097, 1045, 1015 (P–O–C and O–C). ^{1}H-NMR (400 MHz, DMSO-d_6): 1.10 (t, 3H, J = 7.2 Hz, CH_3), 1.29 (t, 3H, J = 7.2 Hz, CH_3), 2.22 (s, 3H, CH_3), 4.01–4.08 (m, 4H, OCH_2), 5.83 (d, 1H, J_{PCH} = 20.4 Hz, P–CH), 7.11 (d, 2H, J = 8.0 Hz, Ar–H), 8.04 (d, 2H, J = 7.6 Hz, Ar–H). ^{13}C-NMR (100 MHz, DMSO-d_6): 13.8 (CH_3), 15.0 (CH_3), 15.9 (CH_3), 48.5 (d, J_{PC} = 155.4 Hz, C-2), 59.5 (OCH_2), 60.6 (OCH_2), 121.4 (C-4_{aryl}), 130.8 (C-$2,6_{aryl}$), 131.7 (C-$3,5_{aryl}$), 136.7 (C-1_{aryl}), 138.3 (C-6), 153.1 (C-5), 163.9 (C-7a), 168.2 (C=O). ^{31}P-NMR (162 MHz, DMSO-d_6): 22.52 ppm. MS (m/z, I%): 444 (M^+, 25%) and 446 (M + 2, 23%). Anal. calcd for $C_{16}H_{18}BrN_2O_4PS$ (445.27): C, 43.16%; H, 4.07%; N, 6.29%; S, 7.20%. Found: C, 43.01%; H, 3.93%; N, 6.11%; S, 7.04%.

3.1.10 2-(4-Chlorophenyl)-3-ethoxy-5-methyl-3-oxido-2*H*-thiazolo[2,3-*e*][1,4,2]diazaphosphole-6-carboxylate (2h). Pale yellow solid obtained after 100 min in an 89% yield (0.88 g), mp 202–203 °C. IR (KBr), (ν max, cm^{-1}): 3085 (C–H_{arom}), 2987, 2931, 2855 (C–H_{aliph}), 1694 (C=O), 1268 (P=O), 1091, 1018 (P–O–C and O–C). ^{1}H-NMR (400 MHz, DMSO-d_6): 1.10 (t, 3H, J = 6.8 Hz, CH_3), 1.19 (t, 3H, J = 6.4 Hz, CH_3), 2.33 (s, 3H, CH_3), 3.95 (q, 2H, J = 6.4 Hz, OCH_2), 4.19 (q, 2H, J = 6.8 Hz, OCH_2), 5.85 (d, 1H, J_{PCH} = 22.0 Hz, P–CH), 7.18 (d, 2H, J = 8.4 Hz, Ar–H), 8.05 (d, 2H, J = 7.6 Hz, Ar–H). ^{13}C-NMR (100 MHz, DMSO-d_6): 14.1 (CH_3), 15.1 (CH_3), 15.9 (CH_3), 49.2 (d, J_{PC} = 154.0 Hz, C-2), 60.6 (OCH_2), 61.4 (OCH_2), 128.5 (C-$3,5_{aryl}$), 131.3 (C-4_{aryl}), 132.2 (C-$2,6_{aryl}$), 137.3 (C-6), 135.2 (C-1_{aryl}), 154.6 (C-5), 163.2 (C-7a), 168.6 (C=O). ^{31}P-NMR (162 MHz, DMSO-d_6): 20.04 ppm. MS (m/z, I%): 399 (M^+, 29%) and 401 (M + 2, 9%). Anal. calcd for $C_{16}H_{18}ClN_2O_4PS$ (400.81): C, 47.95%; H, 4.53%; N, 6.99%; S, 8.00%. Found: C, 47.81%; H, 4.40%; N, 6.86%; S, 7.86%.

3.1.11 3-Ethoxy-5-methyl-2-(4-nitrophenyl)-3-oxido-2*H*-thiazolo[2,3-*e*][1,4,2]diazaphosphole-6-carboxylate (2i). White solid obtained after 100 min in an 88% yield (0.89 g), mp 208–210 °C. IR (KBr), (ν max, cm^{-1}): 3067, 3034 (C–H_{arom}), 2984, 2929, 2908 (C–H_{aliph}), 1702 (C=O), 1272 (P=O), 1097, 1045, 1016 (P–O–C and O–C). ^{1}H-NMR (400 MHz, DMSO-d_6): 1.10 (t, 3H, J = 6.8 Hz, CH_3), 1.22 (t, 3H, J = 6.8 Hz, CH_3), 2.37 (s, 3H, CH_3), 3.92 (q, 2H, J = 6.8 Hz, OCH_2), 4.13 (q, 2H, J = 6.8 Hz, OCH_2), 5.68 (dd, 1H, J_{PCH} = 22.8 and 9.6 and Hz, P–CH), 8.16 (d, 2H, J = 8.4 Hz, Ar–H), 8.41 (d, 2H, J = 8.4 Hz, Ar–H). ^{13}C-NMR (100 MHz, DMSO-d_6): 13.3 (CH_3), 15.1 (CH_3), 16.0 (CH_3), 49.2

(d, J_{PC} = 154.0 Hz, C-2), 59.8 (OCH_2), 61.3 (OCH_2), 123.4 (C-3,5$_{aryl}$), 129.5 (C-2,6$_{aryl}$), 137.1 (C-6), 142.0 (C-1$_{aryl}$), 143.3 (C-4$_{aryl}$), 153.8 (C-5), 163.6 (C-7a), 168.3 (C=O). ^{31}P-NMR (162 MHz, DMSO-d_6): 21.01 ppm. MS (*m*/*z*, *I*%): 411 (M^+, 35%). Anal. calcd for $C_{16}H_{18}N_3O_6PS$ (411.37): C, 46.72%; H, 4.41%; N, 10.21%; S, 7.79%. Found: C, 46.56%; H, 4.28%; N, 10.06%; S, 7.64%.

3.1.12 3-Ethoxy-5-methyl-3-oxido-2-(2,4,6-trimethoxyphenyl)-2*H*-thiazolo[2,3-*e*][1,4,2]diazaphosphole-6-carboxylate (2j). Yellow solid obtained after 120 min in an 81% yield (0.91 g), mp 131–132 °C. IR (KBr), (*ν* max, cm^{-1}): 3034 (C–H$_{arom}$), 2982, 2940, 2908 (C–H$_{aliph}$), 1698 (C=O), 1263 (P=O), 1090, 1014 (P–O–C and O–C). ^{1}H-NMR (400 MHz, DMSO-d_6): 1.10–1.19 (m, 6H, CH_3), 2.36 (s, 3H, CH_3), 3.72 (s, 3H, OCH_3), 3.76 (s, 3H, OCH_3), 3.86 (s, 3H, OCH_3), 4.00–4.15 (m, 4H, OCH_2), 5.85 (d, 1H, J_{PCH} = 20.4 Hz, P–CH), 7.17 (s, 1H, Ar–H), 7.78 (s, 1H, Ar–H). ^{13}C-NMR (100 MHz, DMSO-d_6): 14.0 (CH_3), 15.7 (CH_3), 16.0 (CH_3), 49.8 (d, J_{PC} = 149.1 Hz, C-2), 54.1 (OCH_3), 55.8 (2 OCH_3), 60.9 (OCH_2), 62.3 (OCH_2), 93.5 (C-3,5$_{aryl}$), 106.7 (C-1$_{aryl}$), 138.7 (C-6), 154.7 (C-5), 160.2 (C-2,6$_{aryl}$), 161.5 (C-4$_{aryl}$), 163.4 (C-7a), 166.5 (C=O). ^{31}P-NMR (162 MHz, DMSO-d_6): 20.05 ppm. MS (*m*/*z*, *I*%): 456 (M^+, 100%). Anal. calcd for $C_{19}H_{25}N_2O_7PS$ (456.45): C, 50.00%; H, 5.52%; N, 6.14%; S, 7.02%. Found: C, 49.87%; H, 5.42%; N, 6.03%; S, 6.90%.

3.2 *In vitro* cytotoxicity

The American type of culture collection (ATCC) provided human cell lines for the human cancer cells TK-10 and A549. A humidified, 5% (v/v) CO_2 atmosphere was used to culture the cells at 37 °C in RPMI-1640 supplemented with (100 μg mL^{-1}), penicillin (100 units/mL), and heat-inactivated fetal bovine serum (10% v/v). Using the sulforhodamine B (SRB) assay, the cytotoxicity of the synthesized compounds against TK-10 and A549 human tumor cells was assessed before being treated with the synthesized compounds.[40]

3.3 Apoptosis analysis

The TK-10 and A549 cancer cells were treated for 48 h with the products **2e**, **2h**, and **2j** before being trypsinized and subjected to two PBS washes. According to the manufacturer, apoptosis was evaluated using Alexa Fluor-488/PI staining apoptosis.[41]

3.4 Cell cycle analysis

The IC_{50} values for the products **2e**, **2h**, and **2j** were pre-calculated and administered to TK-10 and A549 cells for 48 h. For the distribution of the cell cycle phases for each sample, FACS analysis was completed using a Cytek® Northern Lights 2000 spectral flow cytometer (Cytek Biosciences, Fremont, CA, USA).[42]

3.5 Autophagy assessment

Autophagic cell death was quantitatively assessed using acridine orange lysosomal staining coupled with flow cytometric analysis. After treatment with the test compounds for the specified duration, cells (105 cells) were collected by trypsinization and washed twice with ice-cold PBS (pH 7.4). The cells were then stained with acridine orange (10 μM) and incubated in the dark at 37 °C for 30 min. After staining, the cells were then subjected to FACS analysis using a Cytek® Northern Lights 2000 spectral flow cytometer and SpectroFlo™ software version 2.2.0.3 (Cytek Biosciences, Fremont, CA, USA).[43]

4. Conclusion

In summary, we have reported a straightforward protocol for the construction of ethyl 2-aryl-3-ethoxy-5-methyl-3-oxido-2*H*-thiazolo[2,3-*e*][1,4,2]diazaphosphole-6-carboxylates. The main features of this work are the protocol is less time-consuming, inexpensive, offers a simple procedure and easy handling, and the derivatives can be obtained in high yields. Compounds that have methoxy groups and chlorine atoms displayed promising cytotoxic activities.

Data availability

All data are available in the manuscript and ESI.†

Author contributions

Data curation: AAS. Formal analysis: AAS. Investigation: TEA, WAB, MYA and SEIE. Writing-original draft: TEA, MAA and WAB. Conceptualization: TEA, MAA and WAB. Supervision: TEA. Resources: TEA, WAB and SEIE. Software: TEA and SEIE. Methodology: WAB and SEIE. Writing – review & editing: TEA, MAA, WAB and SEIE. All authors read and approved the final version of the manuscript.

Conflicts of interest

Authors declare that they have no conflict of interest.

Acknowledgements

The authors extend their appreciation to University Higher Education Fund for funding this research work under Research Support Program for Central Labs at King Khalid University through the Project Number CL/PRI/B/6.

References

1 S. J. Kashyap, V. J. Garg, P. K. Sharma, N. Kumar, R. Dudhe and J. K. Gupta, Thiazoles: having diverse biological activities, *Med. Chem. Res.*, 2012, **21**, 2123.
2 C. A. Calderón-Ospina and M. O. Nava-Mesa, B Vitamins in the nervous system: current knowledge of the biochemical modes of action and synergies of thiamine, pyridoxine, and cobalamin, *CNS Neurosci. Ther.*, 2020, **6**, 5.
3 M. Bagheri, M. Shekarchi, M. Jorjani, M. H. Ghahremani, M. Vosooghi and A. Shafiee, Synthesis and Antihypertensive Activity of 1-(2-Thiazolyl)-3,5-

disubstituted-2-Pyrazolines, *Arch. Pharm. Chem. Life Sci.*, 2004, **337**, 25–34.

4 G. M. Reddy, J. R. Garcia, V. H. Reddy, A. M. Andrade Jr, A. Camilo, R. A. P. Ribeiro and S. R. Lazaro, Synthesis, antimicrobial activity and advances in structure-activity relationships (SARs) of novel tri-substituted thiazole derivatives, *Eur. J. Med. Chem.*, 2016, **123**, 508–515.

5 N. Siddiqui and W. Ahsan, Triazole incorporated thiazoles as a new class of anticonvulsants: design, synthesis and in vivo screening, *Eur. J. Med. Chem.*, 2010, **45**, 1536–1543.

6 S. Anuradha, R. Patel, P. Patle, A. Parameswaran and J. A. Shard, Design, computational studies, synthesis and biological evaluation of thiazole-based molecules as anticancer agents, *Eur. J. Pharm. Sci.*, 2019, **134**, 20–30.

7 M. H. M. Helal, M. A. Salem, M. S. A. El-Gaby and M. Aljahdali, Synthesis and biological evaluation of some novel thiazole compounds as potential anti-inflammatory agents, *Eur. J. Med. Chem.*, 2013, **65**, 517–526.

8 P. Singh, S. Gupta and S. Kumar, Thiazole Compounds as Antiviral Agents: An Update, *Med. Chem.*, 2020, **16**, 4–23.

9 V. Jaishree, N. Ramdas, J. Sachin and B. Ramesh, In vitro antioxidant properties of new thiazole derivatives, *J. Saudi Chem. Soc.*, 2012, **16**, 371–376.

10 R. G. Kalkhambkar, G. M. Kulkarni, H. Shivkumar and R. N. Rao, Synthesis of novel triheterocyclic thiazoles as anti-inflammatory and analgesic agents, *Eur. J. Med. Chem.*, 2007, **42**, 1272–1276.

11 T. K. Venkatachalam, E. A. Sudbeck, C. Mao and F. M. Uckun, Anti-HIV activity of aromatic and heterocyclic thiazolyl thiourea compounds, *Bioorg. Med. Chem. Lett.*, 2001, **11**, 523–528.

12 F. Delmas, A. Avellaneda, C. D. Giorgio, M. Robin, E. D. Clercq, P. Timon-David and J. P. Galy, Synthesis and antileishmanial activity of (1,3-benzothiazol-2-yl)amino-9-(10H)-acridinone derivatives, *Eur. J. Med. Chem.*, 2004, **39**, 685–690.

13 K. Moonen, I. Laureyn and C. V. Stevens, Synthetic Methods for Azaheterocyclic Phosphonates and their Biological Activity, *Chem. Rev.*, 2004, **104**, 6177–6216.

14 V. Iaroshenko and S. Mkrtchyan, Phosphorus Heterocycles, *Organophosphorus Chem.*, 2019, 295–456.

15 G. Keglevich, Newer Developments in the Synthesis of P-Heterocycles, *Curr. Org. Chem.*, 2019, **23**, 1342–1355.

16 A. Schmidpeter, Heterophospholes, *Phosphorus-Carbon Heterocyclic Chemistry*, 2001, pp. 363–461.

17 V. R. Katla, R. Syed, C. S. Kuruva, H. K. Kuntrapakam and N. R. Chamarthi, Synthesis of Novel Phosphorylated Guanidine Derivatives from Cyanamide and their Anti-inflammatory Activity, *Chem. Pharm. Bull.*, 2013, **61**, 25–32.

18 M. Golla, S. R. Devineni, R. Syed, B. K. Rayalacheru, R. Maram and N. R. Chamarthi, New substituted 2-aminomethyl-2-oxo-2λ^5-perhydro-[1,3,2]oxazaphospholo [3,4-a] pyridine: design, synthesis and antimicrobial activity, *Phosphorus, Sulfur Silicon Relat. Elem.*, 2017, **192**, 794–798.

19 W. M. Abdou, M. D. Khidre, A. A. Kamel and G. E. A. Awad, Facile regioselective synthesis and antimicrobial activity of heterocycle-phosphor esters, *Monatsh. Chem.*, 2014, **145**, 675–682.

20 T. E. Ali, M. A. Assiri, H. M. El-Shaaer, S. M. Abed-Kariem, W. R. Abdel-Monem, S. M. El-Edfawy, N. M. Hassanin, A. A. Shati, M. Y. Alfaifi and S. E. I. Elbehairi, Synthesis and Biological Activities of Some New Phosphorus Compounds Containing Pyranopyrazole Moiety, *Heterocycles*, 2021, **102**, 1119–1137.

21 T. E. Ali and M. A. Assiri, One-Pot synthesis and antimicrobial of novel 6-ethoxy-6-oxido-3-oxo(thioxo)(imino)-5-substituted-2,7-dihydro-1,2,4-triazolo [3,4-e][1,2,3]diazaphospholes, *Phosphorus, Sulfur Silicon Relat. Elem.*, 2021, **196**, 965–969.

22 T. E. Ali and M. A. Assiri, Novel 5-Ethoxy-5H-5λ5-[1,2,4] triazolo[5,1-e][1,4,2] diazaphosphol-5-ones: One-Pot Synthesis, Characterization and Antimicrobial Activities, *Russ. J. Org. Chem.*, 2022, **58**, 94–98.

23 T. E. Ali, M. A. Assiri, A. Y. Alzahrani and M. A. Salem, Simple One-Pot Synthesis of Novel 5-(3,5-Dialkyl-1H-pyrazol-1-yl)-2-ethoxy-1,4,2λ^5-diazaphosphole 2-Oxides, *Russ. J. Org. Chem.*, 2023, **59**, 285–289.

24 R. K. Bansal, K. Karaghiosoff and A. Schmidpeter, Anellated heterophospholes, *Tetrahedron*, 1994, **50**, 7675–7745.

25 R. K. Bansal, R. Mahnot, D. C. Sharma and K. Karaghiosoff, Synthesis of New Heterocycles with Dicoordinated Phosphorus: 3-Substituted Thiazolo[3,2-d][1,4,2] diazaphosphole and its 5,6-Dihydro and Benzo Derivatives, *Synthesis*, 1992, 267–269.

26 C. Hettstedt, W. Betzl and K. Karaghiosoff, Synthesis and Characterization of (–)-Menthyl Containing N-Alkyl Cycloimmonium Salts, *Z. Anorg. Allg. Chem.*, 2012, **638**, 377–382.

27 K. Karaghiosoff, R. Mahnot, C. Cleve, N. Gandhi, R. K. Bansal and A. Schmidpeter, 1,4,2-Diazaphospholothiazoles and -pyridines by a Hantzsch-Type Condensation Using Chloromethyldichlorophosphane, *Chem. Ber.*, 1995, **128**, 581–587.

28 W. Betzl, C. Hettstedt and K. Karaghiosoff, New anellated 4H-1,4,2-diazaphospholes, *New J. Chem.*, 2013, **37**, 481–487.

29 T. E. Ali, M. A. Assiri and N. M. Hassanin, Reaction of 1-(2-Hydroxyphenyl)-3-Phenylpropane-1,3-Dione with Some Phosphorus Halides: A Simple Synthesis of Novel 1,2-Benzoxaphosphinines, *Synth. Commun.*, 2022, **52**, 2334–2343.

30 T. E. Ali, M. A. Assiri and N. M. Hassanin, One-Pot Synthesis, Antimicrobial Activities and Drug-Likeness Analysis of Some Novel 1,2-Benzoxa-phosphinines, Phospholo-benzofuran, and Chromonyl/Coumarinyl/Indenonyl Phosphonate, *Synth. Commun.*, 2022, **52**, 1967–1980.

31 T. E. Ali and M. A. Ultrasound, Assisted One Pot, Three-Component Reaction For Facile Design Of Novel Assiri, 1,2,3-Diazaphosphole, 1,5,2-Diazaphosphinine And 1,5,2-Diazaphosphepine Compounds Containing Coumarin Ring, *Heterocycles*, 2022, **104**, 1573–1583.

32 D. A. Bakhotmah, T. E. Ali, M. A. Assiri and I. S. Yahia, Synthesis of some novel 2-{pyrano[2,3-c]pyrazoles-4-ylidene}malononitrile fused with pyrazole, pyridine,

pyrimidine, diazepine, chromone, pyrano[2,3-c]pyrazole and pyrano[2,3-d]pyrimidine systems as anticancer agents, *Polycyclic Aromat. Compd.*, 2022, **42**, 2136.

33 M. Narender, M. S. Reddy, V. P. Kumar, B. Srinivas, R. Sridhar, Y. V. D. Nageswar and K. R. Rao, Aqueous-Phase One-Pot Synthesis of 2-Aminothiazole- or 2-Aminoselenazole-5-carboxylates from β-Keto Esters, Thiourea or Selenourea, and N-Bromo-succinimide under Supramolecular Catalysis, *Synthesis*, 2007, 3469–3472.

34 B. Banerjee, Recent developments on ultrasound assisted catalyst-free organic synthesis, *Ultrason. Sonochem.*, 2017, **35**, 1–14.

35 B. Banerjee, Recent developments on ultrasound-assisted synthesis of bioactive N-heterocycles at ambient temperature, *Aust. J. Chem.*, 2017, **70**, 872–888.

36 Q. Q. Zhang and R. C. Jin, The Application of Low-Intensity Ultrasound Irradiation in Biological Wastewater Treatment: A Review, *Crit. Rev. Environ. Sci. Technol.*, 2015, **45**, 2728–2761.

37 E. Bálint, Á. Tajti, A. Ádám, I. Csontos, K. Karaghiosoff, M. Czugler, P. Ábrányi-Balogh and G. Keglevich, The synthesis of α-aryl-α-aminophosphonates and α-aryl-α-aminophosphine oxides by the microwave-assisted Pudovik reaction, *Beilstein J. Org. Chem.*, 2017, **13**, 76–86.

38 A. J. Rao, P. V. Rao, V. K. Rao, C. Mohan, C. N. Raju and C. S. Reddy, Microwave Assisted One-pot Synthesis of Novel α-Aminophosphonates and their Biological Activity, *Bull. Korean Chem. Soc.*, 2010, **31**, 1863–1868.

39 S. Hkiri, M. Mekni-Toujani, E. Üstün, K. Hosni, A. Ghram, S. Touil, A. Samarat and D. Sémeril, Synthesis of Novel 1,3,4-Oxadiazole-Derived α-Aminophosphonates/α-Aminophosphonic Acids and Evaluation of their In vitro Antiviral Activity against the Avian Coronavirus Infectious Bronchitis Virus, *Pharmaceutics*, 2023, **15**, 114.

40 A. Mahmoud, A. M. Al-Abd, D. A. Lightfoot and H. A. El-Shemy, Anticancer characteristics of mevinolin against three different solid tumor cell lines was not solely p53-dependent, *J. Enzyme Inhib. Med. Chem.*, 2012, **27**, 673–679.

41 S. W. Fesik, Promoting apoptosis as a strategy for cancer drug discovery, *Nat. Rev. Cancer*, 2005, **5**, 876–885.

42 R. Nunez, DNA measurement and cell cycle analysis by flow cytometry, *Curr. Issues Mol. Biol.*, 2001, **3**, 67–70.

43 P. Czarny, E. Pawlowska, J. Bialkowska-Warzecha, K. Kaarniranta and J. Blasiak, Autophagy in DNA Damage Response, *Int. J. Mol. Sci.*, 2015, **16**, 2641–2662.